Transdisciplinary Insights in Life Sciences

ISSN: 2584-2161(Online)
Journal Homepage: www.panainool.com

RESEARCH ARTICLE

Structural, Optical and electrochemical properties of Mo Doped TiO_2 Thin Films Deposited by Spray Pyrolysis technique

Jayaraman Kamalakkannan[1], & B. Sharmila Indirani[2*]

[1]PG & Research Department of Chemistry, Sri Vinayaga College of Arts & science, Ulundurpet – 606 107, Tamil Nadu, India.
*[*2]PG & Research Department of Chemistry, Periyar Arts College, Cuddalore-1, Tamil Nadu, India.*

ARTICLE HISTROY

Received 01 March 2024
Revised 15 March 2024
Accepted 30 March 2024

Keywords
Morphological study
Optical
Electrical properties

ABSTRACT

In the present study, thin films of TiO_2 and Mo-doped TiO_2 were subjected to the SP-spray pyrolysis process at a temperature of 400°C on a glass substrate. We utilized the UV-VIS-NIR spectrophotometer to investigate several optical properties of the thin films, such as the extinction coefficient, absorption coefficient, refractive index, and band gap energy. The measurements were conducted within the photon wavelength range of 300–1200 nm. The band gap exhibited an increase from 3.15 to 3.3 eV when the content of Mo rose from 0% to 12%. The increase in Mo content resulted in a decrease in the transmittance and refractive index of the Mo-doped TiO_2 thin films, respectively. The HR-SEM and HR-TEM examinations reveal that the microstructures and content of the film consist of uniformly distributed nanospherical grains with homogeneous and dense surfaces. This indicates that the film's small-sized grains, which possess a porous nature, are highly suitable for solar cell applications. The energy-dispersive spectroscopy (ED) spectra confirmed that the Mo content in the Mo-doped TiO_2 thin films went up and then down, with less Ti and O. The bare and doped films underwent annealing at a temperature of 500°C for duration of 2 hours. When it comes to the shat circuit, natural dye-sensitized sun cells (DSSCs) produce current that is 0–12% higher than that of TiO_2 thin films, which are man-made dye-sensitized solar cells used in photovoltaic applications.

✉ B. Sharmila Indirani
chemsharmi@gmail.com

Introduction

Titanium dioxide has been intensively researched in many polymorphic forms, such as anatase, rutile, and brookite, for its uses in electrochemistry, photocatalysis, solar cells, self-cleaning surfaces, solid oxide fuel cells, gas sensors, and other fields. This research has spanned over the past three decades (Armaković et al., 2023). Among the several polymorphic forms, anatase has demonstrated superior efficacy in certain applications compared to other

polymorphs (Eddy et al., 2023; Hadjiivanov & Klissurski, 1996). Consequently, it is required to synthesize a single-phase anatase and adjust its features to suit its practical application. Anatase TiO_2 has a band gap of 3.2 electron volts (eV).

In order to customize the wide band gap and render it responsive to visible light, researchers have employed different methodologies, including cation doping and anion doping (Hussain et al., 2023; Li et al., 2016). By doping metals in an adequate amount, it becomes possible to modify the optical bandgap by adjusting the Burstein-Moss (B-M) energy level shift, which is dependent on the concentration of carriers (Zhou et al., 2023).

Nevertheless, in recent years, metal oxide structures have been subjected to doping with Nb, V, Mo, and W elements as substitute cations, and their impacts on metal oxide have been investigated. The element molybdenum (Mo) is found in various oxidation states, one of which is Mo^{6+} (Kumaravel et al., 2020). Various methods have been investigated for the production of nanocrystalline titania thin films, such as sol-gel, screen-printing, dip-coating, chemical vapor deposition, and ultrasonic spray pyrolysis (Dundar et al., 2019; Hamukwaya et al., 2022; Lukong et al., 2022). The ultrasonic spray pyrolysis technique has garnered significant attention due to its straightforwardness, cost-efficiency, and user-friendly nature in the production of TiO_2 thin films (Poostforooshan et al., 2023).

In this study, the ultrasonic spray pyrolysis technique was employed to fabricate thin coatings of TiO_2 on substrates made of silicon and microscope glass. This work employs it based on the analysis of existing literature. The investigation of Mo-doped TiO_2 thin films and the examination of their diverse physical properties continue to be a captivating area of research that warrants effective exploration. Consequently, this study involved the production of TiO_2 thin films doped with Mo at different concentrations to gain a deeper understanding of their structural, electrical, and optical characteristics.

Materials and Method

Component of Explorations

A Sigma Aldrich supplies provided the initial chemicals used in this investigation, which included tetraisopropyl orthotitanate, ammonium molybdate, glacial acetic acid, hydrochloric acid (HCl), ITO-coated glass deionized, and ethanol. We employed glassware that had undergone chromic acid cleansing and subsequent thorough washing with distilled water during the investigations.

Deposited thin films of TiO_2 and Mo-doped TiO_2 onto a glass substrate after chemically cleaning and drying it with acetone and distilled water, and then ultrasonic cleaning it. We carried out this process using a straightforward spray pyrolysis (SP) approach (Dundar et al., 2019). The working solution was prepared by dissolving tetrasopropyl orthotitanate with ammonium molybdate in water at room temperature. We adjusted the source material concentrations to increase Mo doping in TiO_2 by a range of 3%, 6%, 9%, and 12%. The experimental procedure involved maintaining a distance of around 25 cm between the spray nozzle and the substrate. Additionally, we regulated the flow rate of the solution during spraying to approximately 3 mL/min, which remained constant throughout the experiment. The duration of their deposition was 10 minutes. The temperature of the substrate was approximately 4000°C, and it was measured using a copper-constantine thermocouple that was specifically calibrated to achieve films of high quality. Following the deposition process, the samples were permitted to undergo natural cooling until reaching room temperature. The characterization and application were used to estimate the phases of the thin films.

Film Characterization

The structural features of the materials were investigated using a Bruker AXS D8 X-ray diffractometer, with Cu-K radiation of wavelength 1.5405A0 serving as the source. Properties of light the optical characteristics, including absorption and transmission spectra within the 200–2000 nm range were measured using a Varian Carry 5000

UV–Vis–NIR spectrophotometer. A Carl Zeiss EVO MA 15 scanning electron microscope (SEM) examines the surface appearance and grain size of the films. The Stylus technique yielded a thickness range of 85 to 90 nm for the films.

Results and Discussion

Scanning Electron Microscopy (SEM)

Scanning electron microscopy is employed to analyze the uniform distribution of Mo-doped TiO_2 thin film grains (Halin et al., 2021). The resulting film surface consists of small particles that cover the whole substrate region, simulating a granular surface. Figure 1a clearly shows that there is cubic crystal roughness in the area, which means that the spherical grains are spread out evenly and the surfaces are dense and uniform. This characteristic is advantageous for solar cell applications (Xue et al., 2020). Furthermore, the excessive Mo content leads to the segregation of grains. Therefore, we can deduce that Mo significantly influences the surface structure of the film. Figure 1b illustrates the occurrence of Mo, Ti, and O in Mo-doped TiO_2 thin films, as observed in the EDS spectrum.

HR-TEM

In order to conduct a more comprehensive analysis of the morphology, plot profile, surface plot, internal structure, and particle size of the Mo-doped TiO_2 thin film, transmission electron microscopy (TEM) was employed (Cuadra et al., 2023; Esposito et al., 2021). The images were captured at a resolution of 20 nm. TEM images of the film can be obtained because it is expected to have a temperature of 4000 °C and contains a nanobundle spherical structure.

The form of the polycrystalline nature of the thin film is clearly depicted in Figure 2a, which illustrates the impact of Mo doping at a concentration of 9 percent on the crystal planes. Figures 2b, 2c, and 2d depict a plot profile and plot profile 2D interaction, respectively, illustrating an interactive 3D image. The surface plots in the spectrum of the thin film structure and Figure 2e indicate that the mean particle size was 16 nm, while Figure 2a displays the specific particle chosen. The photos demonstrate that the majority of the particles exhibit elongation. Nevertheless, there has been a minor particle aggregation found in the pure samples of thin film. It has been discovered that, despite the aggregation of nanoparticles, they exhibit a limited range of sizes. Furthermore, all previous HR-TEM designs exhibited a crystallite size that closely matched those obtained through the utilization of Scherer's equation.

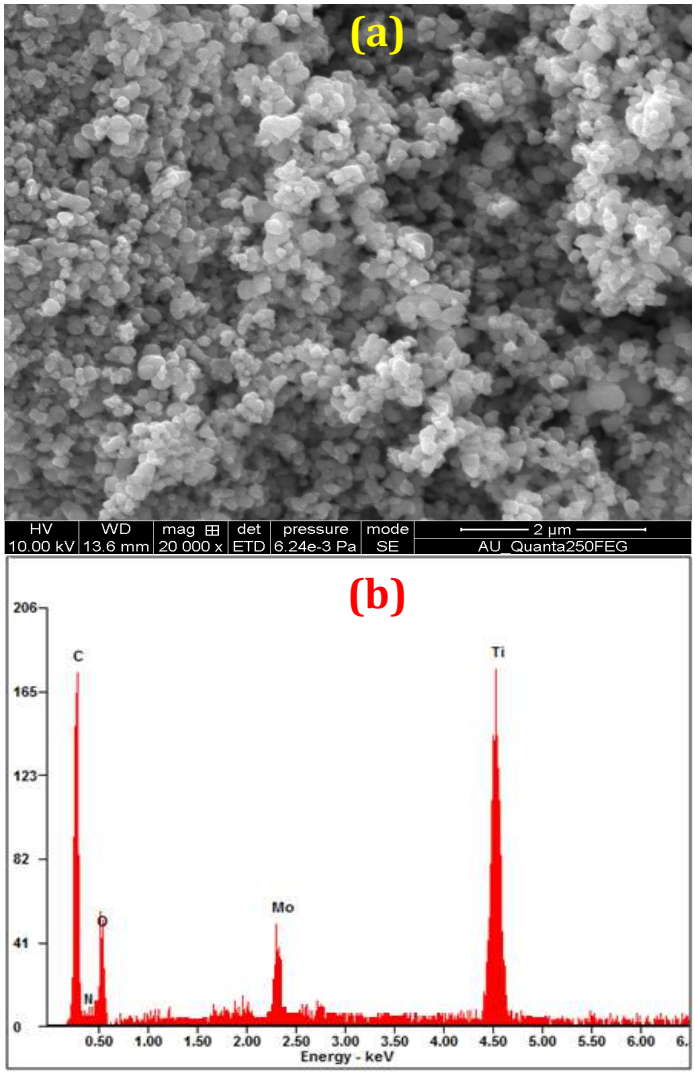

Figure 1. HR-SEM analysis; (a) SEM image of Mo doped TiO_2 (9%) thin film and (b) EDS analysis

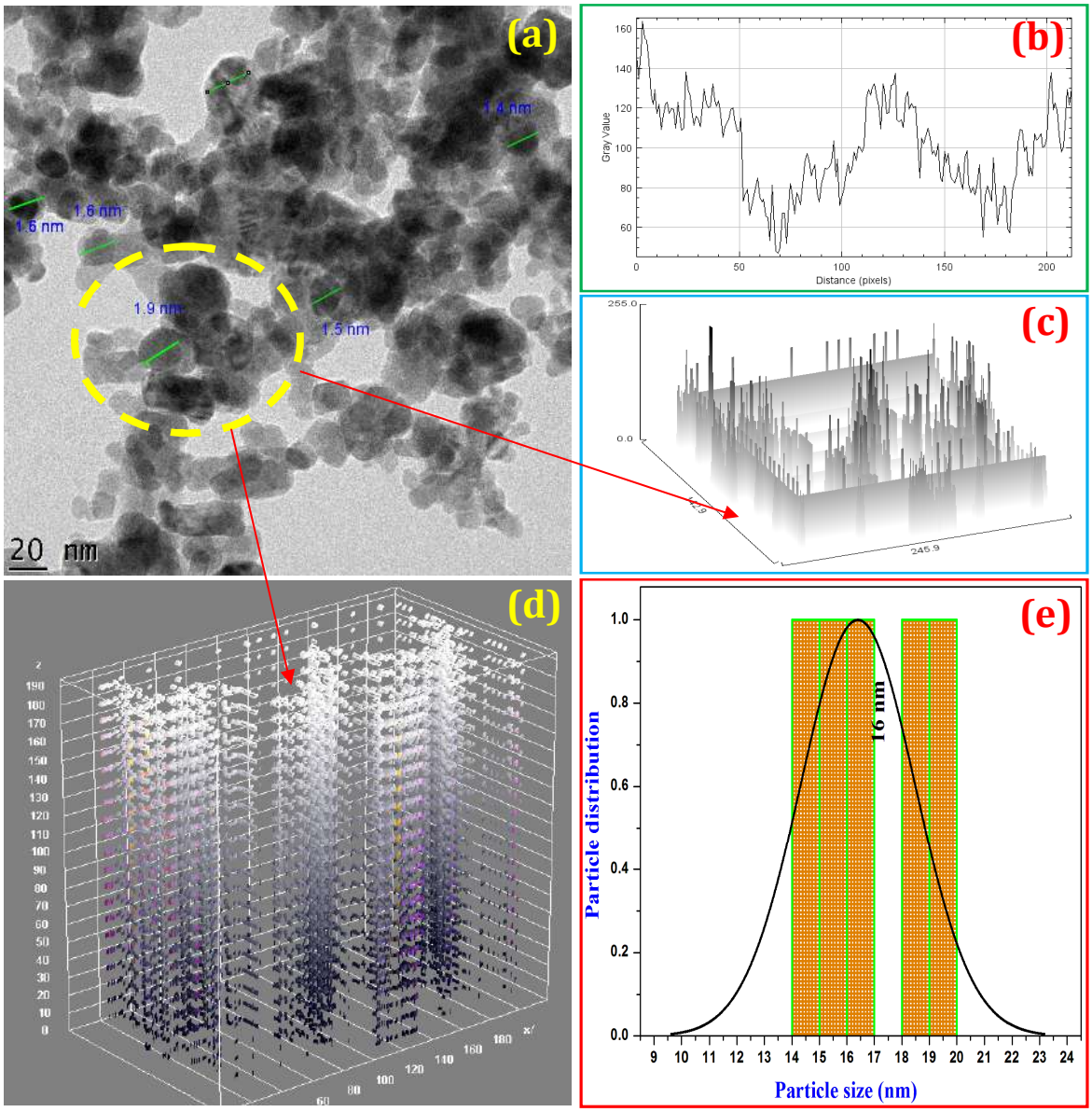

Figure 2. HR-TEM analysis of (a) Image Mo doped TiO_2 (9%) thin film, (b) Plot profile, (c) Plot profile 2D, (d) Interactive 3D-Surface plot spectrum and (e) size in a specific area Figure that has been emphasized (a) a really thin film

Optical investigations

The optical investigations focus on the transmittance spectra of TiO_2 and Mo-doped TiO_2 thin films in the visible and near-infrared regions. The optical properties of these films exhibit significant transmission within the wavelength range of 300–1200 nm. The average transmittance of TiO_2 exceeded 75%, and it increased by 9% with the addition of Mo doping concentration. This can be attributed to the disorder of the films, resulting in an enhanced average transmittance of up to 90% for all films. This indicates high and superior active transmittance. The rise in transmittance can be attributed to the dimensions of the films that have undergone well-crystallization. A high level of transparency is linked to strong structural uniformity and crystallinity (Ahmad et al., 2022). Hence, a thin film of TiO_2 doped with 9 atomic percent (at. %) is deemed appropriate for a range of applications, including the development of transparent conductive films for optoelectronic devices and the production of antireflection coating materials. The increase in Mo content at

12% may result in a decrease in transmittance at higher doping levels. This drop can be attributed to the enhanced scattering of photons caused by crystal defects resulting from doping, as depicted in Figure 3 a–e (Kot et al., 2021).

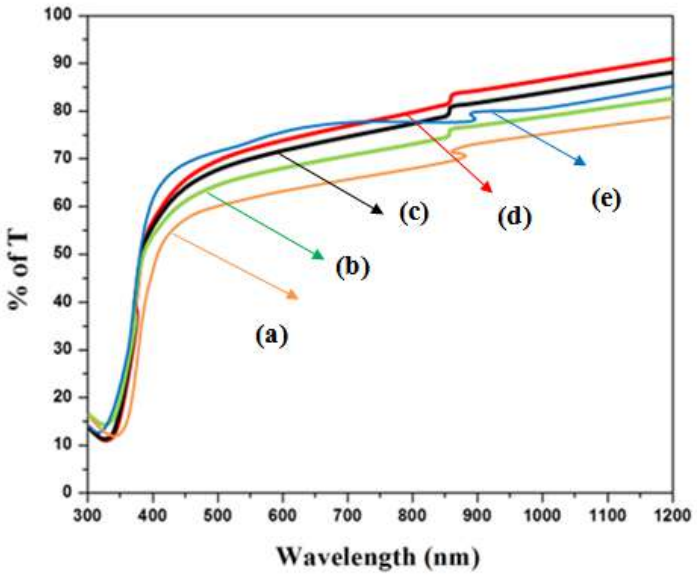

Figure 3. Transmittance (a) TiO_2, (b) Mo-TiO_2 (3%), (c) Mo-TiO_2 (6%), (d) Mo-TiO_2 (9%), and (e) Mo-TiO_2 (12%) thin films.

The observed drop in transmittance as the Mo concentration increases may be attributed to the scattering caused by pores and other flaws within the films. The increased transparency achieved by the film in the visible range indicates its potential use in electrochemical applications for solar devices. The relationship between the combination coefficients -αhν and photon energy –hν for direct transition can be expressed as

$$\alpha h\nu = A\,(h\nu - Eg)^n$$

Where, A represents a constant. The band gap frequency, denoted as Eg, significantly impacts the quality of the transition for both direct and indirect transitions, namely for 1/2 and 2, respectively. The graphs in Figure 4 (a–e) depict the relationship between $(h\nu)^2$ and h. Increasing the concentration of Mo doping from 0-9% leads to a decrease in the band gap energy, causing it to shrink from 3.12 eV to 3.2 eV. This decrease in band gap energy is more pronounced when the Mo doping concentration is increased to 12% of the of the film content. Consistent findings are observed when the author asserts that increasing mover focus leads to a reduction in band width and alterations in optical band gaps (Martynow et al., 2020). The decrease in band gap of 0-9% compared to 12% Mo doping concentration in thin films is attributed to alterations in film solidity and grain extent, resulting in the formation of better and more effective active thin films.

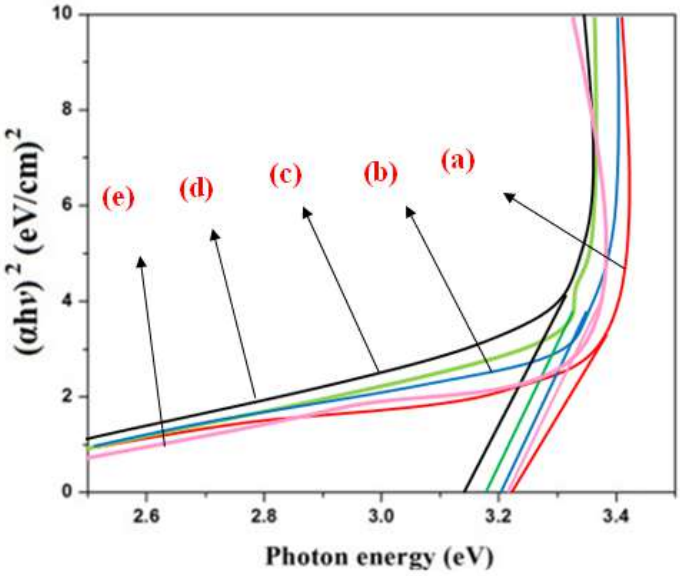

Figure 4. $(\alpha h\nu)^2$ versus Photon energy of plots; (a) TiO_2, (b) Mo-TiO_2 (3%), (c) Mo-TiO_2 (6%), (d) Mo-TiO_2 (9%), and (e) Mo-TiO_2 (12%) thin films.

Extinction coefficient

The Extinction coefficient (k) can be obtained calculated from the relation,

$$k = \frac{\alpha\lambda}{4\pi}$$

Figure 5 shows how the extinction coefficient (k) changes with wavelength for thin films made of pure TiO_2 and Mo-doped TiO_2. We observe a reduction in the extinction coefficient as the wavelength increases. The low extinction coefficient values provide evidence of the exceptional surface smoothness shown by the thin films. The absorption of light at grain boundaries is responsible for the decrease in the extinction coefficient (K) value. The low extinction coefficient values observed in the doped films suggest a high level of homogeneity for Mo concentrations ranging from 0% to 9% (Wang et al., 2020). There is a close correlation between the extinction coefficient (k) and light absorption.

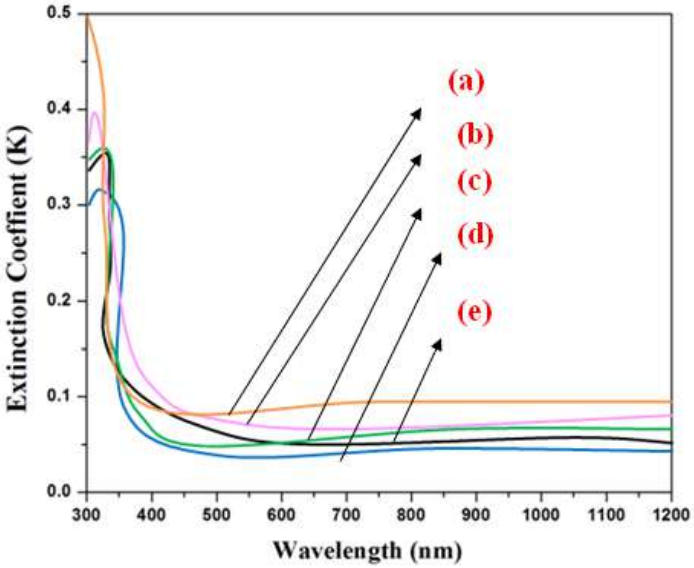

Figure 5. Extinction coefficient of grown various % of ratio (a) TiO_2, (b) Mo-TiO_2 (3%), (c) Mo-TiO_2 (6%), (d) Mo-TiO_2 (9%) and (e) Mo-TiO_2 (12%) thin films

The calculation of the refractive index for different wavelengths in the characterization process is determined by the equation

$$n = \frac{1+R^{1/2}}{1-R^{1/2}}.$$

The study observed an enhancement in the clean and superior active compactness of the TiO_2 films with a Mo doping concentration ranging from 0% to 9%. The refractive index of Mo-doped TiO_2 films exhibits a drop in average value from 0-9%, as depicted in Figure 5 (a–e). The optical density of the film may have decreased due to the application of a 9% Mo-doped TiO_2 thin layer.

Photoluminescence

The photoluminescence spectra of TiO_2 and Mo-doped TiO_2 thin films at 0% to 12% are illustrated in Figures 6a–e. All films exhibit a pronounced near-band edge emission (NBE). The NBE emissions found at 390 nm for TiO_2 are a result of the recombination of free excitons, whereas the green emission at 525 nm is linked to the presence of oxygen vacancies. The film's crystallinity, which increases as the density of defects decreases, is strongly correlated with the film's luminous properties. The film exhibits a TiO_2 crystallinity ranging from 0 to 9% and is doped with 12% Mo. The absence of green release suggests a reduction in O vacancies and an enhancement in crystallinity (Kumaravel et al., 2020; Piątkowska et al., 2021).

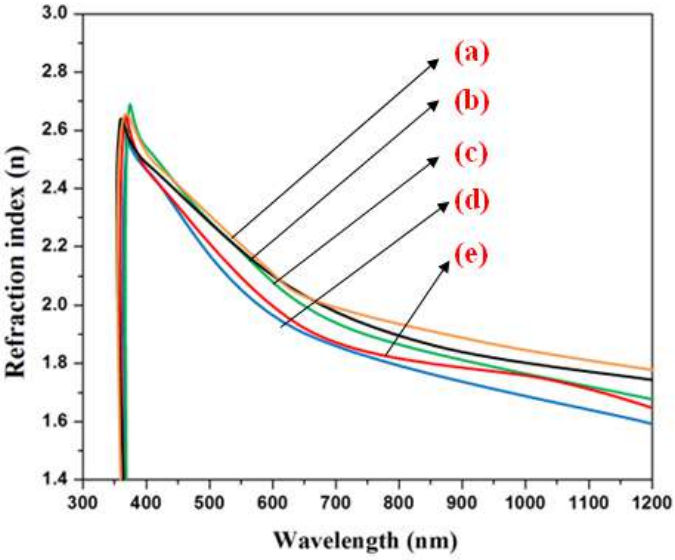

Figure 6. Photoluminescence of grown various % of ratio (a) TiO_2, (b) Mo-TiO_2 (3%), (c) Mo-TiO_2 (6%), (d) Mo-TiO_2 (9%) and (e) Mo-TiO_2 (12%) thin films.

Electrical utilization

DSSCs utilizing natural dyes

The figures illustrate the photocurrent voltage [J-V] characteristics of dye-sensitized solar cells [DSSCs]. The TiO_2 and Mo-doped TiO_2 thin films, created at concentrations ranging from 0 to 12%, serve as photo electrodes. These films are then coated onto FTO-plate glass at different percentages, known as a-e and b-e, using TiO_2 and Mo-doped TiO_2. The TiO_2 and Mo-doped TiO_2 thin films, which were created and incorporated with a natural dye for yellow rose extract (a combination of cyanin 3-glycoside and cyanin 3-rutinoside for anthocyanin dyes), were utilized in the fabrication of the solar cell. By employing dye as a sensitizer, the 9% Mo-doped TiO_2 thin film exhibits the highest values of Jsc (joint short-circuit current output), Voc (500 mV), fill factor (FF), and productivity (g) compared to TiO_2, 3%, 6%, and 12% Mo-doped TiO_2 thin films, which have Jsc values of 6.6, 7, 7.55, and 7.8 mA/cm^2, respectively (Liu et al., 2022). This is illustrated in Figures 7a–e. Consequently, the voltage generated by natural dye-sensitive solar cells (DSSCs) placed over a 9%

Mo-doped TiO_2 thin film (Jsc) (8.0 mA/cm^2) was found to be higher when compared.

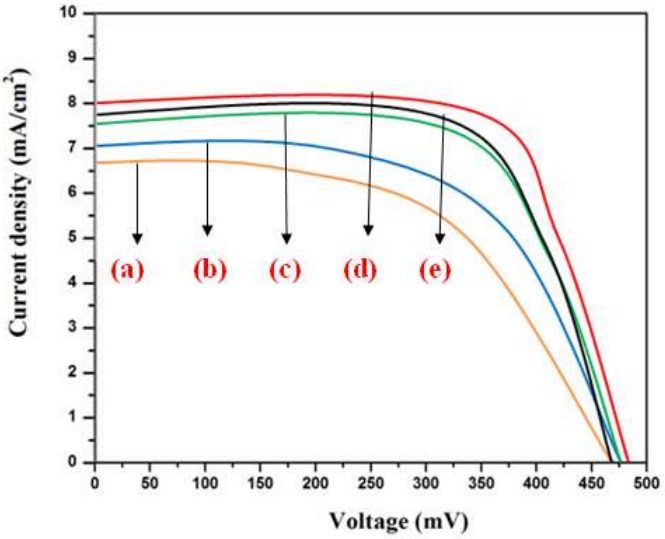

Figure 7. Current density voltage [J–V] curves for the DSSC's fabricated from ratio (a) TiO_2 film GCE, (b) Mo-TiO_2 (3%) film GCE, (c) Mo-TiO_2 (6%) film GCE, (d) Mo-TiO_2 (9%) film GCE and (e) Mo-TiO_2 (12%) film GCE thin films by synthetic dye analysis.

Conclusion

A thin film of TiO_2 and Mo-doped TiO_2 was fabricated by the spray pyrolysis method at a temperature of 400 °C. The Mo concentrations used in the process were 3 at. %, 6 at. %, 9 at. %, and 12 at. %. The resulting film consisted of nano-spherical grains. The EDS spectrum reveals the existence of Mo, Ti, and O in titanium dioxide (TiO_2) sheets doped with Mo. The optical transmittance exhibited an upward trend as the doping ratio increased, while the optical band gap saw a downward trend. The doped film exhibited enhanced minimum resistivity, maximum carrier concentration, and Hall mobility, rendering it suitable for many applications, including gas sensors, optoelectronics, and window layers in solar cells, when applied as a coating over an ITO glass plate. The application section of this study demonstrates that natural dye-sensitive solar cells (DSSCs) exhibit a higher current generation in the shat circuit when utilizing Mo-doped TiO_2 (9%) films compared to doped TiO_2 and Mo-doped TiO_2 (3, 6, and 12%) thin films in manufactured dye-sensitive solar cells. This observation enhances the suitability of these films for optical applications.

Acknowledgement

The authors are thankful to Department of Chemistry, Sri Vinayaga College of Arts & science, Ulundurpet for providing the facilities.

Conflict of interest

All authors declare no conflict of interest.

References

Ahmad, Y. H., Abu Hatab, A. S., Mohamed, A. T., Al-Kuwari, M. S., Aljaber, A. S., & Al-Qaradawi, S. Y. (2022). Microwave-Assisted Solvothermal Synthesis of Mo-Doped TiO(2) with Exceptional Textural Properties and Superior Adsorption Kinetics. *Nanomaterials (Basel, Switzerland)*, *12*(12). https://doi.org/10.3390/nano12122051

Armaković, S. J., Savanović, M. M., & Armaković, S. (2023). Titanium Dioxide as the Most Used Photocatalyst for Water Purification: An Overview. *Catalysts*, *13*(1). https://doi.org/10.3390/catal13010026

Cuadra, J. G., Molina-Prados, S., Mínguez-Vega, G., Estrada, A. C., Trindade, T., Oliveira, C., Seabra, M. P., Labrincha, J., Porcar, S., Cadena, R., Fraga, D., & Carda, J. B. (2023). Multifunctional silver-coated transparent TiO2 thin films for photocatalytic and antimicrobial applications. *Applied Surface Science*, *617*, 156519. https://doi.org/https://doi.org/10.1016/j.apsusc.2023.156519

Dundar, I., Krichevskaya, M., Katerski, A., & Acik, I. O. (2019). TiO 2 thin films by ultrasonic spray pyrolysis as photocatalytic material for air purification. *Royal Society Open Science*, *6*(2). https://doi.org/10.1098/rsos.181578

Eddy, D. R., Permana, M. D., Sakti, L. K., Sheha, G. A. N., Solihudin, Hidayat, S., Takei, T., Kumada, N., & Rahayu, I. (2023). Heterophase Polymorph of TiO(2) (Anatase, Rutile, Brookite, TiO(2) (B)) for Efficient Photocatalyst: Fabrication and Activity. *Nanomaterials (Basel, Switzerland)*, *13*(4). https://doi.org/10.3390/nano13040704

Esposito, S., Ditaranto, N., Dell'Agli, G., Nasi, R., Rivolo, P., & Bonelli, B. (2021). Effective

Inclusion of Sizable Amounts of Mo within TiO2 Nanoparticles Can Be Obtained by Reverse Micelle Sol–Gel Synthesis. *ACS Omega*, *6*(8), 5379–5388. https://doi.org/10.1021/acsomega.0c05552

Hadjiivanov, K. I., & Klissurski, D. G. (1996). Surface chemistry of titania (anatase) and titania-supported catalysts. *Chem. Soc. Rev.*, *25*(1), 61–69. https://doi.org/10.1039/CS9962500061

Halin, D. S. C., Razak, K. A., Mohd Salleh, M. A. A., Ramli, M. I. I., Abdullah, M. M. A. B., Azhari, A. W., Nogita, K., Yasuda, H., Nabiałek, M., & Wysłocki, J. J. (2021). Microstructure Evolution of Ag/TiO2 Thin Film. *Magnetochemistry*, *7*(1). https://doi.org/10.3390/magnetochemistry7010014

Hamukwaya, S. L., Hao, H., Zhao, Z., Dong, J., Zhong, T., Xing, J., Hao, L., & Mashingaidze, M. M. (2022). A Review of Recent Developments in Preparation Methods for Large-Area Perovskite Solar Cells. *Coatings*, *12*(2). https://doi.org/10.3390/coatings12020252

Hussain, A., Rauf, A., Ahmed, E., Khan, M. S., Mian, S. A., & Jang, J. (2023). Modulating Optoelectronic and Elastic Properties of Anatase TiO(2) for Photoelectrochemical Water Splitting. *Molecules (Basel, Switzerland)*, *28*(7). https://doi.org/10.3390/molecules28073252

Kot, A., Radecka, M., Dorosz, D., & Zakrzewska, K. (2021). Optically Active TiO(2):Er Thin Films Deposited by Magnetron Sputtering. *Materials (Basel, Switzerland)*, *14*(15). https://doi.org/10.3390/ma14154085

Kumaravel, V., Rhatigan, S., Mathew, S., Michel, M. C., Bartlett, J., Nolan, M., Hinder, S. J., Gascó, A., Ruiz-Palomar, C., Hermosilla, D., & Pillai, S. C. (2020). Mo doped TiO2: impact on oxygen vacancies, anatase phase stability and photocatalytic activity. *Journal of Physics: Materials*, *3*(2), 25008. https://doi.org/10.1088/2515-7639/ab749c

Li, L., Meng, F., Hu, X., Qiao, L., Sun, C. Q., Tian, H., & Zheng, W. (2016). TiO2 Band Restructuring by B and P Dopants. *PloS One*, *11*(4), e0152726. https://doi.org/10.1371/journal.pone.0152726

Liu, Y., Chen, J., Tian, Z., & Yao, J. (2022). Dye-Sensitized Solar Cell Based on TiO(2) Anode Thin Film with Three-Dimensional Web-like Structure. *Materials (Basel, Switzerland)*, *15*(17). https://doi.org/10.3390/ma15175875

Lukong, V. T., Mouchou, R. T., Enebe, G. C., Ukoba, K., & Jen, T. C. (2022). Deposition and characterization of self-cleaning TiO2 thin films for photovoltaic application. *Materials Today: Proceedings*, *62*, S63–S72. https://doi.org/10.1016/j.matpr.2022.02.089

Martynow, M., Głowienka, D., Galagan, Y., & Guthmuller, J. (2020). Effects of Bromine Doping on the Structural Properties and Band Gap of CH3NH3Pb(I1–xBrx)3 Perovskite. *ACS Omega*, *5*(41), 26946–26953. https://doi.org/10.1021/acsomega.0c04406

Piątkowska, A., Janus, M., Szymański, K., & Mozia, S. (2021). C-,N- and S-Doped TiO2 Photocatalysts: A Review. *Catalysts*, *11*(1). https://doi.org/10.3390/catal11010144

Poostforooshan, J., Belbekhouche, S., Olszok, V., Stodt, M. F. B., Simmler, M., Bierwirth, M., Nirschl, H., Kiefer, J., Fritsching, U., & Weber, A. P. (2023). Synthesis of Pure and Fe-Doped TiO2 Nanoparticles via Electrospray-Assisted Flame Spray Pyrolysis for Antimicrobial Applications. *ACS Applied Nano Materials*, *6*(24), 22660–22672. https://doi.org/10.1021/acsanm.3c03107

Wang, Y.-H., Rahman, K. H., Wu, C.-C., & Chen, K.-C. (2020). A Review on the Pathways of the Improved Structural Characteristics and Photocatalytic Performance of Titanium Dioxide (TiO2) Thin Films Fabricated by the Magnetron-Sputtering Technique. *Catalysts*, *10*(6). https://doi.org/10.3390/catal10060598

Xue, D., Luo, J., Li, Z., Yin, Y., & Shen, J. (2020). Enhanced Photoelectrochemical Properties from Mo-Doped TiO2 Nanotube Arrays Film. *Coatings*, *10*(1). https://doi.org/10.3390/coatings10010075

Zhou, X., Huang, E., Zhang, R., Xiang, H., Zhong, W., & Xu, B. (2023). Multicolor Tunable Electrochromic Materials Based on the Burstein–Moss Effect. *Nanomaterials*, *13*(10). https://doi.org/10.3390/nano13101580